# Secrecy performance analysis of single-input multiple-output generalized-$K$ fading channels[*][#]

Hong-jiang LEI[†1,2], Imran Shafique ANSARI[3], Chao GAO[†‡2], Yong-cai GUO[2],

Gao-feng PAN[4], Khalid A. QARAQE[3]

(*[1]Chongqing Key Laboratory of Mobile Communications Technology, Chongqing University of*
*Posts and Telecommunications, Chongqing 400065, China*)

(*[2]MOE Key Laboratory of Optoelectronic Technology and Systems, Chongqing University, Chongqing 400044, China*)

(*[3]Department of Electrical and Computer Engineering, Texas A&M University at Qatar, Doha, Qatar*)

(*[4]Chongqing Key Laboratory of Nonlinear Circuits and Intelligent Information Processing,*
*Southwest University, Chongqing 400715, China*)

[†]E-mail: leihj@cqupt.edu.cn; chaogaocqu@126.com

Received Mar. 8, 2016;  Revision accepted July 6, 2016;  Crosschecked Sept. 11, 2016

**Abstract:**    In this paper, the transmission of confidential messages through single-input multiple-output (SIMO) independent and identically generalized-$K$ ($K_G$) fading channels is considered, where the eavesdropper overhears the transmission from the transmitter to the receiver. Both the receiver and the eavesdropper are equipped with multiple antennas, and both active and passive eavesdroppings are considered where the channel state information of the eavesdropper's channel is or is not available at the transmitter. The secrecy performance of SIMO $K_G$ systems is investigated. Analytical expressions for secrecy outage probability and average secrecy capacity of SIMO systems are derived via two different methods, in which $K_G$ distribution is approximated by the Gamma and mixture Gamma distributions, respectively. Numerical results are presented and verified via the Monte-Carlo simulation.

**Key words:**  Physical-layer security, Generalized-$K$ fading, Average secrecy capacity, Secrecy outage probability, Mixture Gamma distribution

http://dx.doi.org/10.1631/FITEE.1601070                    **CLC number:**  TN918.8

---

# 1  Introduction

## 1.1  Background

Composite fading channels, such as Rayleigh-lognormal (RL) and Nakagami-lognormal (NL) distributions, have been frequently used to model shadowing and multipath fading that occur simultaneously in realistic wireless scenarios (Stuber, 2011). However, the probability density function (PDF) of such lognormal-based fading models is not given in a closed form, which makes the performance analysis difficult or even intractable (Jung *et al.*, 2014). Hence, several channel models with closed-form PDF have been proposed to represent wireless propagation properties, such as the $K$ distribution (Abdi

and Kaveh, 1998; Bithas and Rontogiannis, 2015), generalized-$K$ ($K_{\mathrm{G}}$) distribution (Shankar, 2004), and $\mathcal{G}$-distribution (Laourine *et al.*, 2009). Among these, $K_{\mathrm{G}}$ distribution has been used quite extensively as can be seen from the open literature, and the reason behind this is the fact that various fading scenarios are covered in the closed form within the $K_{\mathrm{G}}$ distribution simply by adjusting two parameters (Shankar, 2004). For example, the performance of two-way amplify-and-forward (AF) relaying systems over cascaded $K_{\mathrm{G}}$ fading channels was analyzed by Yadav and Upadhyay (2013), and the expressions for both upper and lower bounds for outage probability were derived.

Traditional communications use cryptographic encryption and decryption methods in the upper layers of wireless network protocol stacks to provide information security. Differing from the traditional approach, physical-layer security was identified as a promising strategy that offers secure communication by smartly exploiting the fading of the channels (Yang *et al.*, 2015). Recently, extensive efforts have been devoted to exploring the physical-layer secrecy performance over fading channels. Ata and Altunbaş (2015) analyzed the relay antenna selection problem in a vehicle-to-vehicle communication system employing physical-layer network coding with the AF scheme and obtained the lower and upper bounds of the end-to-end signal-to-noise ratio (SNR) and the cumulative density functions (CDFs). The secrecy performance of the classic Wyner's wiretap model over the generalized Gamma fading channels was analyzed, and the closed-form expressions for the probability of strictly positive secrecy capacity (SPSC) and the lower bound of secrecy outage probability (SOP) were derived by Lei *et al.* (2015b). The performance of secure communications over non-small-scale fading channels was investigated, and approximate closed-form expressions for the average secrecy capacity (ASC), SOP, and SPSC over independent log-normal fading, correlated log-normal fading, and independent composite fading channels were derived by Pan *et al.* (2016). Zou *et al.* (2013; 2015a) proposed several optimal relay selection schemes to improve the physical-layer security in wireless cooperative networks and cognitive radio networks, respectively. Zou *et al.* (2015b) presented several diversity techniques for improving wireless security against eavesdropping attacks. The secrecy outage prob-

ability and diversity performances of a multi-user multi-eavesdropper cellular network were studied by Jiang *et al.* (2015). Liu *et al.* (2016) investigated the secrecy performance of cognitive radio systems over Rayleigh and log-normal fading channels in the presence of one eavesdropper, and derived exact and approximate closed-form expressions for the SOP. However, no study focuses on the physical-layer security over $K_{\mathrm{G}}$ fading channels. Based on results of Al-Ahmadi and Yanikomeroglu (2010b) and Chatzidiamantis and Karagiannidis (2011), Lei *et al.* (2015a) studied the secrecy performance over single-input multiple-output (SIMO) $K_{\mathrm{G}}$ fading channels and derived the closed-form expressions for the ASC, the bound of the SOP, and the SPSC. Through modeling the SNR over $K_{\mathrm{G}}$ channels with a mixture Gamma (MG) distribution, Lei *et al.* (2016a) analyzed the secrecy performance for the classic Wyner's model over $K_{\mathrm{G}}$ fading channels.

### 1.2 Motivation and contributions

In this study, the secrecy performance of SIMO $K_{\mathrm{G}}$ systems is investigated. The main contributions of our work are listed as follows:

1. In the first method, the sum of independent $K_{\mathrm{G}}$ random variables (RVs) is approximated by a Gamma RV, and new expressions for the ASC, the bound of the SOP, and the SPSC over SIMO $K_{\mathrm{G}}$ fading channels are derived.

2. In the second method, the $K_{\mathrm{G}}$ distribution is approximated by the MG distribution, and new closed-form expressions for ASC and SOP over SIMO $K_{\mathrm{G}}$ fading channels are derived.

3. The asymptotic SOP, the secrecy diversity order, and the secrecy array gain are derived.

These novel expressions provide a unified form that can handle several of the well-known composite fading environments as special or limiting cases. The two methods demonstrated in our work will be a helpful reference for researchers dealing with $K_{\mathrm{G}}$ fading channels, especially with the physical-layer security issues in $K_{\mathrm{G}}$ fading scenarios.

## 2 System model

We consider a wiretap radio network, in which the transmitter ($S$) communicates with the legitimate receiver ($D$) under the malicious attempt of the eavesdropper ($E$), as shown in Fig. 1. It is

assumed that $S$ is equipped with a single antenna, and $D$ and $E$ are equipped with $N_D$ ($N_D \geq 1$) and $N_E$ ($N_E \geq 1$) antennas, respectively. Furthermore, we assume that both the main and eavesdropper channels undergo independent and identically distributed (i.i.d.) quasi-static $K_G$ fading. The PDF and CDF of the SNR over a $K_G$ channel are respectively given by (Bithas *et al.*, 2006)

$$f_i(\gamma) = \frac{2\Xi_i^{\frac{\beta_i+1}{2}}}{\Gamma(m_i)\Gamma(k_i)}\gamma^{\frac{\beta_i-1}{2}}K_{\alpha_i}\left(2\sqrt{\Xi_i\gamma}\right), \quad (1)$$

$$F_i(\gamma) = \pi\csc(\pi\alpha_i)$$
$$\cdot\left(\frac{(\Xi_i\gamma)^{m_i}{}_1F_2(m_i;1-\alpha_i,1+m_i;\Xi_i\gamma)}{\Gamma(k_i)\Gamma(1-\alpha_i)\Gamma(1+m_i)}\right.$$
$$\left.-\frac{(\Xi_i\gamma)^{k_i}{}_1F_2(k_i;1+\alpha_i,1+k_i;\Xi_i\gamma)}{\Gamma(m_i)\Gamma(1+\alpha_i)\Gamma(1+k_i)}\right),$$
$$(2)$$

where $\Gamma(\cdot)$ is the Gamma function, $i \in \{D, E\}$, $m_i$ and $k_i$ are the fading parameters of the main and eavesdropper channels respectively, and $\gamma$ is the SNR. Both $m_i$ and $k_i$ are limited to integer values, $\alpha_i = k_i - m_i$, $\beta_i = k_i + m_i - 1$, $\Xi_i = m_i k_i/\bar{\gamma}_i$ with $\bar{\gamma}_i$ being the average SNR of the main and eavesdropper channels, $K_a(\cdot)$ is the modified Bessel function of order $a$, and ${}_pF_q(a;b;c)$ is the generalized hyper-geometric function as defined in Eq. (9.14.2) in Gradshteyn and Ryzhik (2007).
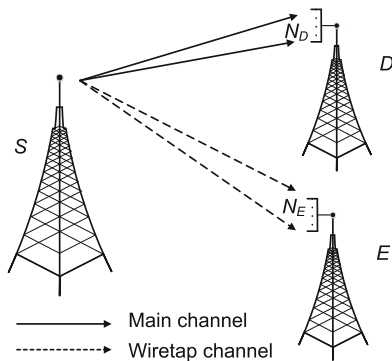


**Fig. 1 System model demonstrating a source ($S$), a legitimate destination ($D$), and an eavesdropper ($E$). The receivers are equipped with multiple antennas**

It is assumed that the maximal radio combining (MRC) scheme is adopted at the destination. Then the instantaneous SNR at $D$ (or $E$) can be expressed as

$$\gamma_i = \sum_{j=1}^{N_i}\gamma_{i,j}, \quad (3)$$

where $i \in \{D, E\}$ and $\gamma_{i,j}$ signifies the instantaneous SNR at the $j$th antenna of $D$ (or $E$).

## 3 Statistical properties

Although the $K_G$ distribution has a closed-form PDF compared with RL and NL distributions, the modified Bessel function (contained in Eq. (1)) makes the performance analysis of $K_G$ channels complicated and difficult. As pointed out in Al-Ahmadi and Yanikomeroglu (2010a) and Atapattu *et al.* (2011), it is not straightforward to deal with the CDF expression (Eq. (2)), which contains the hypergeometric functions, to derive the distributions of $\gamma_i$.

Several methods have been proposed to avoid such difficulties and to significantly simplify the performance analysis of composite fading channels. It was testified that both a single $K_G$ RV and the sum of independent $K_G$ RVs can be closely approximated by a single Gamma RV (Al-Ahmadi and Yanikomeroglu, 2010a). Atapattu *et al.* (2011) proposed an MG distribution to model the SNR of the wireless composite fading channels and analyzed the ergodic capacity of diversity reception schemes over $K_G$ fading channels. The MG distribution is composed of a weighted sum of Gamma distributions that can approximate the $K_G$ distribution as well as a variety of other fading distributions with high accuracy by adjusting its parameters. The high accuracy of this method was testified by Cheng (2013) and Jung *et al.* (2013; 2014). The PDF and CDF via two different methods are given in this section. For simplicity, we refer to these two methods as 'Gamma-based' and 'mixture Gamma-based', respectively.

### 3.1 Gamma-based method

Al-Ahmadi and Yanikomeroglu (2010a) showed that the sum of independent $K_G$ random variables can be approximated by a Gamma RV. The PDF of $\gamma_i$ with the Gamma-based method is given as (Al-Ahmadi and Yanikomeroglu, 2010a)

$$f_i(\gamma) = \frac{\theta_i^{-\rho_i}}{\Gamma(\rho_i)}\gamma^{\rho_i-1}\exp\left(-\frac{\gamma}{\theta_i}\right), \quad (4)$$

where $i \in \{D, E\}$, $\theta_i = (\mathrm{AF}_i - \varepsilon_i)\bar{\gamma}_i$, $\rho_i = \dfrac{N_i}{\mathrm{AF}_i - \varepsilon_i}$, $\mathrm{AF}_i = \dfrac{1}{m_i} + \dfrac{1}{k_i} + \dfrac{1}{m_i k_i}$, and $\varepsilon_i$ is the adjustment parameter (Al-Ahmadi and Yanikomeroglu, 2010a).

Using Eq. (4) above and Eq. (3.351.1) in Gradshteyn and Ryzhik (2007), the CDF of $\gamma_i$ is obtained as

$$F_i(\gamma) = \frac{1}{\Gamma(\rho_i)} \Upsilon\left(\rho_i, \frac{\gamma}{\theta_i}\right), \qquad (5)$$

where $\Upsilon(\alpha, x) = \int_0^x \exp(-t) t^{\alpha-1} \mathrm{d}t$ is the well-known lower incomplete Gamma function, which is defined by Eq. (8.350.1) in Gradshteyn and Ryzhik (2007).

### 3.2 Mixture Gamma-based method

Atapattu et al. (2011) proposed the MG distribution to model the SNR of the $K_{\mathrm{G}}$ channels. The high accuracy of this method was testified by Cheng (2013) and Jung et al. (2013; 2014). The PDF of $\gamma_i$ is derived with the MG-based method in Lemma 1.

**Lemma 1** (Lei et al., 2016b)　The PDF and CDF of $\gamma_i$, $i \in \{D, E\}$ are given by

$$f_i(\gamma) = (\Gamma(m_i))^{N_i} \sum_{S_i} B_i \sum_{j=1}^{L} \sum_{l=1}^{n_{i,j} m_i} \left(\frac{R_{jl}}{(l-1)!}\right.$$
$$\left. \cdot \gamma^{l-1} \exp(-\varsigma_{i,j}\gamma)\right), \qquad (6)$$

$$F_i(\gamma) = (\Gamma(m_i))^{N_i} \sum_{S_i} B_i \sum_{j=1}^{L} \sum_{l=1}^{n_{i,j} m_i} \left(\frac{R_{jl}}{(l-1)!}\right.$$
$$\left. \cdot (\varsigma_{i,j})^{-l} \Upsilon(l, \varsigma_{i,j}\gamma)\right), \qquad (7)$$

where $i \in \{D, E\}$, $R_{jl}$ denotes the coefficient which can be obtained by Eq. (18) in Lei et al. (2016b),

$$B_i = \begin{pmatrix} N_i \\ n_{i,1}, n_{i,2}, \ldots, n_{i,L} \end{pmatrix} \left(\prod_{1 \le j \le L} (\alpha_{i,j})^{n_{i,j}}\right),$$

$$\begin{pmatrix} N_i \\ n_{i,1}, n_{i,2}, \ldots, n_{i,L} \end{pmatrix} = \frac{N_i!}{\prod\limits_{j=1}^{L} (n_{i,j})!},$$

$$S_i = \left\{(n_{i,1}, n_{i,2}, \ldots, n_{i,L}) \left| \sum_{j=1}^{L} n_{i,j} = N_i\right.\right\},$$

$$\alpha_{i,j} = \frac{\theta_{i,j}}{\sum\limits_{v=1}^{L} N\left(\theta_{i,v} \Gamma(m_i)(\varsigma_{i,v})^{-m_i}\right)},$$

$$\varsigma_{i,j} = \frac{\Xi_i}{t_j}, \quad \theta_{i,j} = \frac{\Xi_i^{m_i} \omega_j t_j^{k_i - m_i - 1}}{\Gamma(m_i) \Gamma(k_i)},$$

$\omega_j$ and $t_j$ are the weight factor and the abscissas for the Gaussian–Laguerre integration (Abramowitz

and Stegun, 1972) respectively, and $L$ is the number of terms.

**Lemma 2**　In the high SNR regime with $\bar{\gamma}_D \to \infty$, the asymptotic PDF and CDF of $\gamma_D$ are given by

$$f_D^\infty(\gamma) = \eta \gamma^{m_D N_D - 1}, \qquad (8)$$

$$F_D^\infty(\gamma) = \frac{\eta}{m_D N_D} \gamma^{m_D N_D}, \qquad (9)$$

where $\eta = \dfrac{\lambda^{N_D}(\Gamma(m_D))^{N_D}}{(m_D N_D - 1)!}$ and $\lambda = \sum\limits_{s=1}^{L} \alpha_{D,s}$.

The proof is given in Appendix.

## 4 Average secrecy capacity analysis

In this section, we consider active eavesdropping scenarios, where the full channel state information (CSI) of both the main and eavesdropper channels are available at $S$ (Wang et al., 2014). In such a scenario, $S$ can adapt the achievable secrecy rate $R_{\mathrm{s}}$ such that $R_{\mathrm{s}} \le C_{\mathrm{s}}$, where $C_{\mathrm{s}}$ is the maximum achievable secrecy rate, i.e., secrecy capacity, and can be characterized as (Bloch et al., 2008)

$$C_{\mathrm{s}}(\gamma_D, \gamma_E) = \max\{\ln(1+\gamma_D) - \ln(1+\gamma_E), 0\}, \qquad (10)$$

where $\ln(1+\gamma_D)$ and $\ln(1+\gamma_E)$ are the capacities of the main and eavesdropper channels, respectively.

Then the ASC can be given by

$$\overline{C}_{\mathrm{s}} = \int_0^\infty \int_0^\infty C_{\mathrm{s}}(\gamma_D, \gamma_E) f(\gamma_D, \gamma_E) \, \mathrm{d}\gamma_D \mathrm{d}\gamma_E$$
$$= \underbrace{\int_0^\infty \ln(1+\gamma_D) f_D(\gamma_D) F_E(\gamma_D) \, \mathrm{d}\gamma_D}_{I_1}$$
$$+ \underbrace{\int_0^\infty \ln(1+\gamma_E) f_E(\gamma_E) F_D(\gamma_E) \, \mathrm{d}\gamma_E}_{I_2}$$
$$- \underbrace{\int_0^\infty \ln(1+\gamma_E) f_E(\gamma_E) \, \mathrm{d}\gamma_E}_{I_3}, \qquad (11)$$

where $f(\gamma_D, \gamma_E) = f_D(\gamma_D) f_E(\gamma_E)$ is the joint PDF of $\gamma_D$ and $\gamma_E$.

In the following, we give the derivation of $I_1$, $I_2$, and $I_3$ by using the Gamma-based and MG-based methods.

## 4.1 Gamma-based method

Substituting Eqs. (4) and (5) into Eq. (11), we obtain

$$
\begin{aligned}
I_1 &= \int_0^\infty \ln(1+\gamma_D)\, F_E(\gamma_D)\, f_D(\gamma_D)\, \mathrm{d}\gamma_D \\
&= \frac{\theta_D^{-\rho_D}}{\Gamma(\rho_D)\Gamma(\rho_E)} \\
&\quad \cdot \int_0^\infty \frac{\gamma_D^{\rho_D-1}\ln(1+\gamma_D)}{\exp(\gamma_D/\theta_D)} \Upsilon\left(\rho_E, \frac{\gamma_D}{\theta_E}\right) \mathrm{d}\gamma_D.
\end{aligned}
\tag{12}
$$

By using Eqs. (8) and (9) in Lei *et al.* (2015b) and Eq. (11) in Adamchik and Marichev (1990), the logarithmic, exponential, and incomplete Gamma functions can be expressed in terms of Meijer's G-function as

$$
\ln(1+\gamma_D) = G_{2,2}^{1,2}\left[\gamma_D \,\Big|_{1,0}^{1,1}\right],
\tag{13}
$$

$$
\exp\left(-\frac{\gamma_D}{\theta_D}\right) = G_{0,1}^{1,0}\left[\frac{\gamma_D}{\theta_D} \,\Big|_0^-\right],
\tag{14}
$$

$$
\Upsilon\left(\rho_E, \frac{\gamma_D}{\theta_E}\right) = G_{1,2}^{1,1}\left[\frac{\gamma_D}{\theta_E} \,\Big|_{\rho_E,0}^1\right].
\tag{15}
$$

Using Eq. (9.31.5) in Gradshteyn and Ryzhik (2007), we deduce

$$
\gamma_D^{\rho_D-1} G_{0,1}^{1,0}\left[\frac{\gamma_D}{\theta_D} \,\Big|_0^-\right] = \theta_D^{\rho_D-1} G_{0,1}^{1,0}\left[\frac{\gamma_D}{\theta_D} \,\Big|_{\rho_D-1}^-\right].
\tag{16}
$$

Hence, using Eq. (20) in Lei *et al.* (2015a), we obtain the closed-form expression of $I_1$ in terms of the extended generalized bivariate Meijer's G-function (EGBMGF) as (Ansari *et al.*, 2011)

$$
\begin{aligned}
I_1 &= \frac{\theta_D^{-\rho_D}}{\Gamma(\rho_D)\Gamma(\rho_E)} \theta_D^{\rho_D-1} \int_0^\infty G_{2,2}^{1,2}\left[\gamma_D \,\Big|_{1,0}^{1,1}\right] \\
&\quad \cdot G_{0,1}^{1,0}\left[\frac{\gamma_D}{\theta_D} \,\Big|_{\rho_D-1}^-\right] G_{1,2}^{1,1}\left[\frac{\gamma_D}{\theta_E} \,\Big|_{\rho_E,0}^1\right] \mathrm{d}\gamma_D \\
&= \frac{1}{\Gamma(\rho_D)\Gamma(\rho_E)} \\
&\quad \cdot G_{1,0:2,2:1,2}^{1,0:1,2:1,1}\left(\rho_D \,\Big|_{1,0}^{1,1} \,\Big|_{\rho_E,0}^1 \,\Big|\, \theta_D, \frac{\theta_D}{\theta_E}\right).
\end{aligned}
\tag{17}
$$

Similarly, we obtain the closed-form expression of $I_2$ as

$$
\begin{aligned}
I_2 &= \int_0^\infty \ln(1+\gamma_E)\, f_E(\gamma_E)\, F_D(\gamma_E)\, \mathrm{d}\gamma_E \\
&= \frac{1}{\Gamma(\rho_D)\Gamma(\rho_E)} \\
&\quad \cdot G_{1,0:2,2:1,2}^{1,0:1,2:1,1}\left(\rho_E \,\Big|_{1,0}^{1,1} \,\Big|_{\rho_D,0}^1 \,\Big|\, \theta_E, \frac{\theta_E}{\theta_D}\right).
\end{aligned}
\tag{18}
$$

Now, substituting Eq. (4) into Eq. (9) and using Eqs. (11) and (21) in Adamchik and Marichev (1990), we obtain the closed-form expression of $I_3$ as

$$
\begin{aligned}
I_3 &= \int_0^\infty \ln(1+\gamma_E)\, f_E(\gamma_E)\, \mathrm{d}\gamma_E \\
&= \frac{\theta_E^{-\rho_E}}{\Gamma(\rho_E)} \int_0^\infty \ln(1+\gamma_E)\, \gamma_E^{\rho_E-1} \exp\left(-\frac{\gamma_E}{\theta_E}\right) \mathrm{d}\gamma_E \\
&= \frac{\theta_E^{-\rho_E}}{\Gamma(\rho_E)} \int_0^\infty \gamma_E^{\rho_E-1} G_{2,2}^{1,2}\left[\gamma_E \,\Big|_{1,0}^{1,1}\right] G_{0,1}^{1,0}\left[\frac{\gamma_E}{\theta_E} \,\Big|_0^-\right] \mathrm{d}\gamma_E \\
&= \frac{\theta_E^{-\rho_E}}{\Gamma(\rho_E)} G_{2,3}^{3,1}\left[\frac{1}{\theta_E} \,\Big|_{0,-\rho_E,-\rho_E}^{-\rho_E,1-\rho_E}\right].
\end{aligned}
\tag{19}
$$

Therefore, the ASC is obtained by substituting Eqs. (17)–(19) into Eq. (11).

## 4.2 Mixture Gamma-based method

Substituting Eqs. (6) and (7) into Eq. (11) and using Eq. (21) in Adamchik and Marichev (1990), we obtain

$$
\begin{aligned}
I_1 &= \int_0^\infty \ln(1+\gamma_D)\, f_D(\gamma_D)\, F_E(\gamma_D)\, \mathrm{d}\gamma_D \\
&= A \sum_{S_D} \sum_{S_E} B \sum_{j=1}^{L} \sum_{l=1}^{n_{D,j}m_D} \sum_{s=1}^{L} \sum_{t=1}^{n_{E,s}m_E} \frac{R_{jl}R_{st}\xi_1}{(l-1)!(\varsigma_{E,s})^t},
\end{aligned}
\tag{20}
$$

where $A = (\Gamma(m_D))^{N_D}(\Gamma(m_E))^{N_E}$, $B = B_D B_E$, $R_{jl}$ and $R_{st}$ are coefficients which can be obtained by Eq. (18) in Lei *et al.* (2016b), and

$$
\begin{aligned}
\xi_1 =\, & G_{2,3}^{3,1}\left[\varsigma_{D,j} \,\Big|_{0,-l,-l}^{-l,1-l}\right] \\
& - \sum_{p=0}^{t-1} \frac{(\varsigma_{E,s})^p}{p!} G_{2,3}^{3,1}\left[\varsigma_{D,j}+\varsigma_{E,s} \,\Big|_{0,-l-p,-l-p}^{-l-p,1-l-p}\right].
\end{aligned}
$$

Similarly, we obtain the closed-form expression of $I_2$ as

$$
\begin{aligned}
I_2 &= \int_0^\infty \ln(1+\gamma_E)\, f_E(\gamma_E)\, F_D(\gamma_E)\, \mathrm{d}\gamma_E \\
&= A \sum_{S_D} \sum_{S_E} B \sum_{j=1}^{L} \sum_{l=1}^{n_{D,j}m_D} \sum_{s=1}^{L} \sum_{t=1}^{n_{E,s}m_E} \frac{R_{jl}R_{st}\xi_2}{(t-1)!(\varsigma_{D,j})^l},
\end{aligned}
\tag{21}
$$

where

$$
\begin{aligned}
\xi_2 =\, & G_{2,3}^{3,1}\left[\varsigma_{E,s} \,\Big|_{0,-t,-t}^{-t,1-t}\right] \\
& - \sum_{p=0}^{l-1} \frac{(\varsigma_{D,j})^p}{p!} G_{2,3}^{3,1}\left[\varsigma_{D,j}+\varsigma_{E,s} \,\Big|_{0,-p-t,-p-t}^{-p-t,1-p-t}\right].
\end{aligned}
$$

Now, substituting Eq. (6) into Eq. (11), we obtain

$$
\begin{aligned}
I_3 &= \int_0^\infty \ln\left(1 + \gamma_E\right) f_E\left(\gamma_E\right) \mathrm{d}\gamma_E \\
&= \left(\Gamma\left(m_E\right)\right)^{N_E} \sum_{S_E} B_E \sum_{s=1}^{L} \sum_{t=1}^{n_{E,s} m_E} \frac{R_{st}}{(t-1)!} \\
&\quad \cdot G_{2,3}^{3,1}\left[\varsigma_{E,s} \left| \begin{matrix} -t, 1-t \\ 0, -t, -t \end{matrix} \right. \right].
\end{aligned} \tag{22}
$$

Substituting Eqs. (20)–(22) into Eq. (11), the closed-form expression for the ASC for this scenario is obtained.

# 5 Secrecy outage probability analysis

In this section, we consider passive eavesdropping scenarios, where $S$ has no CSI about the eavesdropper's channel (Wang *et al.*, 2014). In such a scenario, $S$ has no choice but to encode the confidential data into codewords with a constant rate $R_s$ (Wang *et al.*, 2014). If $R_s \leq C_s$, perfect secrecy can be achieved; otherwise, information theoretic security is compromised. The SOP is a useful performance metric to evaluate the secrecy performance of such scenarios, which can be expressed as (Bloch *et al.*, 2008)

$$
\begin{aligned}
P_{\text{out}} &= \Pr\left\{C_s\left(\gamma_D, \gamma_E\right) \leq R_s\right\} \\
&= \Pr\left\{\gamma_D \leq \Theta\gamma_E + \Theta - 1\right\} \\
&= \int_0^\infty F_D\left(\Theta\gamma_E + \Theta - 1\right) f_E\left(\gamma_E\right) \mathrm{d}\gamma_E, \tag{23}
\end{aligned}
$$

where $R_s$ $(R_s \geq 0)$ is the target secrecy capacity threshold and $\Theta = \exp\left(R_s\right) \geq 1$.

## 5.1 Gamma-based method

By substituting Eqs. (4) and (5) into Eq. (23), we obtain

$$
\begin{aligned}
P_{\text{out}} &= \int_0^\infty F_D\left(\Theta\gamma_E + \Theta - 1\right) f_E\left(\gamma_E\right) \mathrm{d}\gamma_E \\
&= \frac{\theta_E^{-\rho_E}}{\Gamma\left(\rho_D\right)\Gamma\left(\rho_E\right)} \\
&\quad \cdot \int_0^\infty \frac{\gamma_E^{\rho_E - 1}}{\exp(\gamma_E/\theta_E)} \Upsilon\left(\rho_D, \frac{\Theta\gamma_E + \Theta - 1}{\theta_D}\right) \mathrm{d}\gamma_E.
\end{aligned} \tag{24}
$$

The integral in Eq. (24) is not available in the exact closed form because of the shift in the incomplete Gamma function $(\rho_i, \ i \in \{D, E\}$ in Eq. (5) is

not an integer). Hence, we derive the lower bound of the SOP by adopting a similar method proposed in Liu (2013) and Lei *et al.* (2015b), i.e.,

$$
\begin{aligned}
P_{\text{out}} &= P\left\{\gamma_D \leq \Theta\gamma_E + \Theta - 1\right\} \\
&\geq P_{\text{out}}{}^{\text{L}} = P\left\{\gamma_D \leq \Theta\gamma_E\right\} \\
&= \int_0^\infty F_D\left(\Theta\gamma_E\right) f_E\left(\gamma_E\right) \mathrm{d}\gamma_E. \tag{25}
\end{aligned}
$$

Now, using Eqs. (4), (5), and Eq. (2.10.3.2) in Prudnikov *et al.* (1992), we obtain the lower bound of the SOP as

$$
\begin{aligned}
P_{\text{out}}^{\text{L}} &= \int_0^\infty F_D\left(\Theta\gamma_E\right) f_E\left(\gamma_E\right) \mathrm{d}\gamma_E \\
&= \frac{\theta_E^{-\rho_E}}{\Gamma\left(\rho_D\right)\Gamma\left(\rho_E\right)} \\
&\quad \cdot \int_0^\infty \frac{\gamma_E^{\rho_E - 1}}{\exp(\gamma_E/\theta_E)} \Upsilon\left(\rho_D, \frac{\Theta\gamma_E}{\theta_D}\right) \mathrm{d}\gamma_E \\
&= \frac{\Gamma\left(\rho_E + \rho_D\right)}{\rho_D\Gamma\left(\rho_E\right)\Gamma\left(\rho_D\right)} \left(\frac{\Theta\theta_E}{\theta_D}\right)^{\rho_D} \\
&\quad \cdot {}_2F_1\left(\rho_D, \rho_E + \rho_D; \rho_D + 1; -\frac{\theta_E\Theta}{\theta_D}\right), \tag{26}
\end{aligned}
$$

where ${}_2F_1\left(a, b; c; z\right)$ is the Gauss hyper-geometric function, as defined in Eq. (9.100) in Gradshteyn and Ryzhik (2007).

## 5.2 Mixture Gamma-based method

By substituting Eqs. (6) and (7) into Eq. (23) and using Eq. (8.352.4) in Gradshteyn and Ryzhik (2007), we obtain

$$
\begin{aligned}
&P_{\text{out}} \\
&= \int_0^\infty F_D\left(\Theta\gamma_E + \Theta - 1\right) f_E\left(\gamma_E\right) \mathrm{d}\gamma_E \\
&= A \sum_{S_D} \sum_{S_E} B \sum_{j=1}^{L} \sum_{l=1}^{n_{D,j} m_D} \sum_{s=1}^{L} \sum_{t=1}^{n_{E,s} m_E} \frac{R_{jl} R_{st} \xi_3}{(t-1)!(\varsigma_{D,j})^l}, \tag{27}
\end{aligned}
$$

where

$$
\begin{aligned}
\xi_3 &= \int_0^\infty \gamma_E^{t-1} \exp\left(-\varsigma_{E,s}\gamma_E\right) \\
&\quad \cdot \left(1 - \sum_{p=0}^{l-1} \frac{(\varsigma_{D,j})^p (\Theta\gamma_E + \Theta - 1)^p}{p! \exp\left(\varsigma_{D,j}\left(\Theta\gamma_E + \Theta - 1\right)\right)}\right) \mathrm{d}\gamma_E. \tag{28}
\end{aligned}
$$

Using Eqs. (1.111) and (3.326.2) in Gradshteyn

and Ryzhik (2007), we obtain

$$
\begin{aligned}
\xi_3 =& \frac{\Gamma(t)}{(\varsigma_{E,s})^t} - \exp(-\varsigma_{D,j}(\Theta-1)) \\
& \cdot \sum_{p=0}^{l-1} \sum_{v=0}^{p} \binom{p}{v} \frac{\Theta^v (\Theta-1)^{p-v} \Gamma(t+v)}{p!(\varsigma_{D,j})^{-p}(\varsigma_{E,s}+\Theta\varsigma_{D,j})^{t+v}},
\end{aligned}
$$

where $\binom{p}{v} = \dfrac{p!}{v!\,(p-v)!}$.

### 5.3 Asymptotic secrecy outage probability

The asymptotic SOP can be expressed as (Wang *et al.*, 2014)

$$
P_{\text{out}}^{\infty} = (G_{\text{a}}\bar{\gamma}_D)^{-G_{\text{d}}} + o\left(\bar{\gamma}_D^{-G_{\text{d}}}\right), \qquad (29)
$$

where $G_{\text{d}}$ refers to the secrecy diversity order, which determines the slope of the asymptotic outage probability curve, and $G_{\text{a}}$ refers to the secrecy array gain, which characterizes the SNR advantage of the asymptotic SOP relative to the reference curve $\bar{\gamma}_D^{-G_{\text{d}}}$.

Substituting Eq. (9) into Eq. (23) and using the multinomial theorem and Eq. (3.326.2) in Gradshteyn and Ryzhik (2007), we obtain

$$
\begin{aligned}
P_{\text{out}}^{\infty} =& \int_0^{\infty} F_D\left(\Theta\gamma_E + \Theta - 1\right) f_E\left(\gamma_E\right) \mathrm{d}\gamma_E \\
=& \frac{\eta(\Gamma(m_E))^{N_E}}{m_D N_D} \sum_{S_E} B_E \sum_{s=1}^{L} \sum_{t=1}^{n_{E,s}m_E} \frac{R_{st}}{(t-1)!} \\
& \cdot \int_0^{\infty} (\Theta\gamma_E + \Theta - 1)^{m_D N_D} \\
& \cdot \gamma_E^{t-1} \exp\left(-\varsigma_{E,s}\gamma_E\right) \mathrm{d}\gamma_E \\
=& \frac{\eta(\Gamma(m_E))^{N_E}}{m_D N_D} \sum_{S_E} B_E \sum_{s=1}^{L} \sum_{t=1}^{n_{E,s}m_E} \frac{R_{st}}{(t-1)!} \xi_3^{\infty},
\end{aligned}
$$
$$(30)$$

where $\xi_3^{\infty} = \displaystyle\sum_{j=0}^{m_D N_D} \binom{m_D N_D}{j} \Theta^j \frac{\Gamma(j+t)}{(\varsigma_{E,s})^{j+t}}$.

Henceforth, based on Eqs. (29) and (30) and the definitions of $\lambda$, $\eta$, the secrecy diversity order and the secrecy array gain are obtained as

$$
G_{\text{d}} = N_D m_D, \qquad (31)
$$

$$
\begin{aligned}
G_{\text{a}} =& \left( \frac{\mu(\Gamma(m_E))^{N_E}}{m_D N_D} \sum_{S_E} B_E \right. \\
& \left. \cdot \sum_{s=1}^{L} \sum_{t=1}^{n_{E,s}m_E} \frac{R_{st}\xi_3^{\infty}}{(t-1)!} \right)^{-\frac{1}{N_D m_D}}, \qquad (32)
\end{aligned}
$$

where

$$
\mu = \frac{(m_D k_D)^{N_D m_D}}{(m_D N_D - 1)!} \left( \frac{\displaystyle\sum_{s=1}^{L}\left(\omega_s(t_s)^{k_D - m_D - 1}\right)}{\displaystyle\sum_{s=1}^{L}\left(\omega_s(t_s)^{k_D - 1}\right)} \right)^{N_D}.
$$

## 6 Strictly positive secrecy capacity analysis

The SPSC (Liu, 2013; Pan *et al.*, 2016), which means the existence of secrecy capacity, is a fundamental benchmark in secure communications, and can be obtained by

$$
P_0 = \Pr\left\{C_{\text{s}}\left(\gamma_D, \gamma_E\right) > 0\right\} = 1 - P_{\text{out}}|_{R_{\text{s}}=0}. \quad (33)
$$

### 6.1 Gamma-based method

By substituting $R_{\text{s}} = 0$ into Eq. (26), we obtain SPSC for this scenario as

$$
\begin{aligned}
P_0 =& 1 - \frac{\Gamma(\rho_D+\rho_E)}{\rho_D\Gamma(\rho_D)\Gamma(\rho_E)} \left(\frac{\theta_E}{\theta_D}\right)^{\rho_D} \\
& \cdot {}_2F_1\left(\rho_D, \rho_D+\rho_E; \rho_D+1; -\frac{\theta_E}{\theta_D}\right). \quad (34)
\end{aligned}
$$

### 6.2 Mixture Gamma-based method

By substituting $R_{\text{s}} = 0$ into Eq. (27), we obtain

$$
\begin{aligned}
P_0 =& 1 - A \sum_{S_D} \sum_{S_E} \left( B \right. \\
& \left. \cdot \sum_{j=1}^{L} \sum_{l=1}^{n_{D,j}m_D} \sum_{s=1}^{L} \sum_{t=1}^{n_{E,s}m_E} \frac{R_{jl}R_{st}\xi_4}{(l-1)!\,(t-1)!} \right),
\end{aligned}
$$
$$(35)$$

where $\xi_4 = \dfrac{\Gamma(t)}{(\varsigma_{E,s})^t} - \displaystyle\sum_{p=0}^{l-1} \frac{(\varsigma_{D,j})^p \Gamma(t+p)}{p!(\varsigma_{D,j}+\varsigma_{E,s})^{t+p}}$.

## 7 Numerical results

In this section, we present numerical results and Monte-Carlo simulations to validate our analysis models. The main parameters used in simulations and analysis are $L = 5$, $m_D = m_E = m$, $k_D = k_E = k$, and the unit of $R_{\text{s}}$ is nat/(s·Hz). The curves under various conditions for comparison with varying $\bar{\gamma}_D$ are plotted.

Figs. 2–8 depict the ASC, SOP, and SPSC versus $\bar{\gamma}_D$ with varying $(N_D, N_E)$, $\bar{\gamma}_E$, and $R_{\text{s}}$ over SIMO

$K_G$ channels, respectively. With the Gamma-based method, we obtain only the lower bound of the SOP and hence the results do not fully agree with the simulations, while the exact SOP can be achieved with the MG-based method. It is clear that the analysis results match very well with simulation curves in all figures except Fig. 8. Furthermore, it can be observed that the ASC, SOP, and SPSC for a higher $\bar{\gamma}_D$ outperform the ones for a lower $\bar{\gamma}_D$ scenario as a higher $\bar{\gamma}_D$ signifies better channel conditions.

As demonstrated in Figs. 2–4, one can find that all the secrecy performance metrics are enhanced by increasing $N_D$ or decreasing $N_E$, which signifies the number of antennas at $D$ or $E$. It can be explained by the fact that $N_D$ and $N_E$ directly influence the receive diversity at $D$ and $E$, respectively. From Figs. 3

and 6, we also observe that the asymptotic results accurately approach the secrecy diversity order and the secrecy array gain. According to Eq. (31), we can observe that the secrecy diversity order is independent of $N_E$ and increases with the increase of $N_D$, which are testified by Fig. 3. As depicted in Figs. 5–7, one can observe that all the secrecy performance metrics are improved while decreasing $\bar{\gamma}_E$, which is the average SNR of the eavesdropper channel. It is because a lower $\bar{\gamma}_E$ signifies weaker eavesdropper channel conditions. In Fig. 8, one can observe that the simulated values for $P_{\text{out}}$ gradually approach the numerical results via the Gamma-based method as $R_s$ decreases, which can be easily explained by $\lim_{R_s \to 0} (\Theta - 1) \to 0$, and very well match the analytical results via the MG-based method.
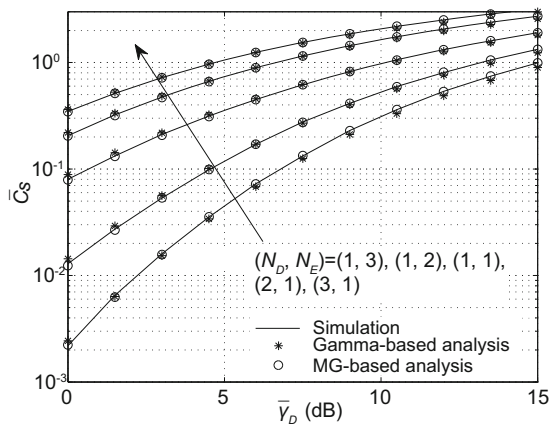


Fig. 2 Average secrecy capacity versus $\bar{\gamma}_D$ with $m = 2$, $R_s = 0.1$, $k = 3$, and $\bar{\gamma}_E = 5$ dB
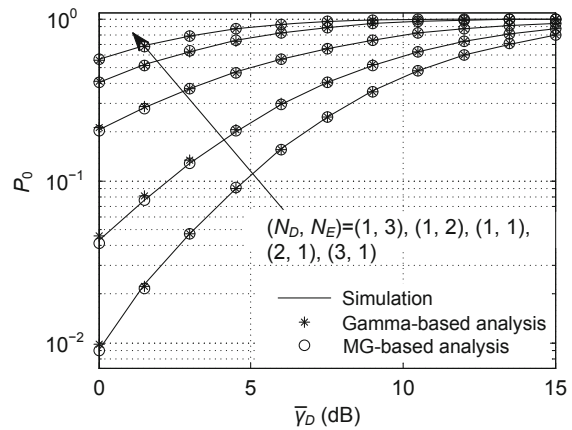


Fig. 4 Strictly positive secrecy capacity versus $\bar{\gamma}_D$ with $m = 2$, $R_s = 0.1$, $k = 3$, and $\bar{\gamma}_E = 5$ dB
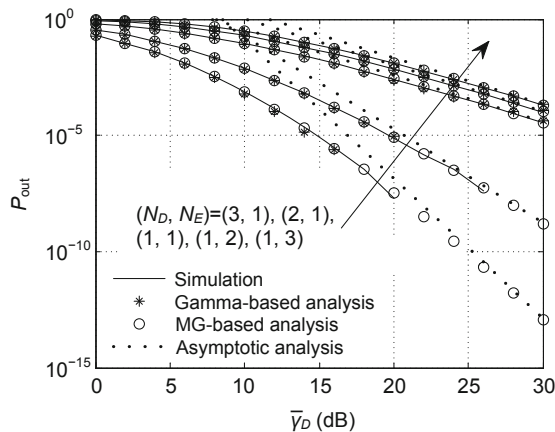


Fig. 3 Secrecy outage probability versus $\bar{\gamma}_D$ with $m = 2$, $R_s = 0.1$, $k = 3$, and $\bar{\gamma}_E = 1$ dB
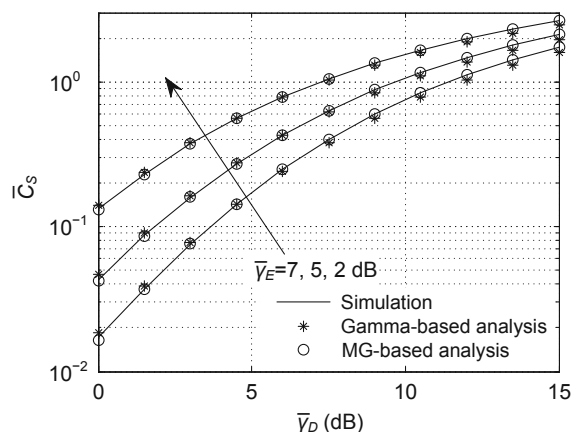


Fig. 5 Average secrecy capacity versus $\bar{\gamma}_D$ with $R_s = 0.1$, $m = 2$, $k = 3$, and $N_D = N_E = 2$
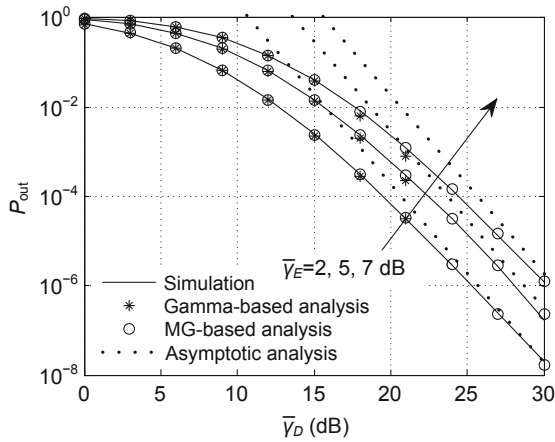
**Fig. 6 Secrecy outage probability versus $\bar{\gamma}_D$ with $R_s = 0.1$, $m = 2$, $k = 3$, and $N_D = N_E = 2$**
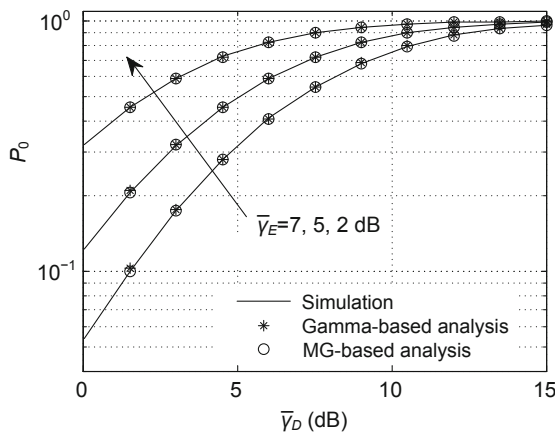


**Fig. 7 Strictly positive secrecy capacity versus $\bar{\gamma}_D$ with $R_s = 0.1$, $m = 2$, $k = 3$, and $N_D = N_E = 2$**
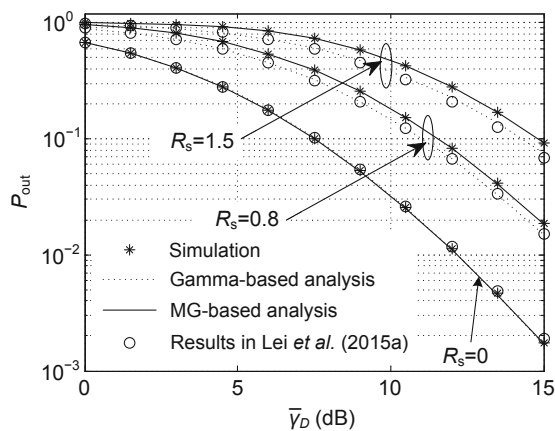


**Fig. 8 Secrecy outage probability versus $\bar{\gamma}_D$ with $m = 2$, $k = 2$, $\bar{\gamma}_E = 2$ dB, and $N_D = N_E = 2$**

# 8 Conclusions

In this paper, the physical-layer security over independent SIMO $K_G$ channels was investigated via two different methods. In the first method, the sum of independent $K_G$ RVs was approximated by a Gamma RV, and new closed-form expressions for the ASC, the bound of the SOP, and the SPSC over SIMO $K_G$ fading channels were derived. In the second method, the $K_G$ distribution was approximated by the MG distribution, and new closed-form expressions for the ASC, SOP, and SPSC were derived. Furthermore, the asymptotic SOP, the secrecy diversity order, and the secrecy array gain were obtained. The model considered in this paper is more general, and it can be applied in various practical application scenarios. For example, a radio cellular wireless communication system is composed of a single antenna mobile station (MS) and a base station (BS) with multiple antennas; another BS equipped with multiple antennas wants to overhear the information from the MS of the legitimate BS. Our results provide a unified model to analyze the secrecy performance over SIMO $K_G$ fading channels and can be readily applied to practical wireless system design, in which the physical-layer security issue is considered.

## References

Abdi, A., Kaveh, M., 1998. K distribution: an appropriate substitute for Rayleigh-lognormal distribution in fading-shadowing wireless channels. *Electron. Lett.*, **34**(9):851-852. http://dx.doi.org/10.1049/el:19980625

Abramowitz, M., Stegun, I.A., 1972. Handbook of Mathematical Functions: with Formulas, Graphs, and Mathematical Tables. Dover Press, New York.

Adamchik, V.S., Marichev, O.I., 1990. The algorithm for calculating integrals of hypergeometric type functions and its realization in REDUCE system. Proc. Int. Symp. on Symbolic and Algebraic Computation, p.212-224. http://dx.doi.org/10.1145/96877.96930

Al-Ahmadi, S., Yanikomeroglu, H., 2010a. On the approximation of the generalized-K distribution by a Gamma distribution for modeling composite fading channels. *IEEE Trans. Wirel. Commun.*, **9**(2):706-713. http://dx.doi.org/10.1109/TWC.2010.02.081266

Al-Ahmadi, S., Yanikomeroglu, H., 2010b. On the approximation of the PDF of the sum of independent generalized-K RVs by another generalized-K PDF with applications to distributed antenna systems. Proc. IEEE Wireless Communications and Networking Conf., p.1-6. http://dx.doi.org/10.1109/WCNC.2010.5506178

Ansari, I.S., Al-Ahmadi, S., Yilmaz, F., et al., 2011. A new formula for the BER of binary modulations with dual-branch selection over generalized-K composite fading channels. *IEEE Trans. Commun.*, **59**(10):2654-2658. http://dx.doi.org/10.1109/TCOMM.2011.063011.100303A

Ata, S.Ö., Altunbaş, İ., 2015. Relay antenna selection for V2V communications using PLNC over cascaded fading channels. Proc. Int. Wireless Communications and Mobile Computing Conf., p.1336-1340. http://dx.doi.org/10.1109/IWCMC.2015.7289276

Atapattu, S., Tellambura, C., Jiang, H., 2011. A mixture Gamma distribution to model the SNR of wireless channels. *IEEE Trans. Wirel. Commun.*, **10**(12):4193-4203. http://dx.doi.org/10.1109/TWC.2011.111210.102115

Bithas, P.S., Rontogiannis, A.A., 2015. Mobile communication systems in the presence of fading/shadowing, noise and interference. *IEEE Trans. Commun.*, **63**(3):724-737. http://dx.doi.org/10.1109/TCOMM.2015.2390625

Bithas, P.S., Sagias, N.C., Mathiopoulos, P.T., *et al.*, 2006. On the performance analysis of digital communications over generalized-$K$ fading channels. *IEEE Commun. Lett.*, **10**(5):353-355. http://dx.doi.org/10.1109/LCOMM.2006.1633320

Bloch, M., Barros, J., Rodrigues, M.R.D., *et al.*, 2008. Wireless information-theoretic security. *IEEE Trans. Inform. Theory*, **54**(6):2515-2534. http://dx.doi.org/10.1109/TIT.2008.921908

Chatzidiamantis, N.D., Karagiannidis, G.K., 2011. On the distribution of the sum of Gamma-Gamma variates and applications in RF and optical wireless communications. *IEEE Trans. Commun.*, **59**(5):1298-1308. http://dx.doi.org/10.1109/TCOMM.2011.020811.090205

Cheng, W., 2013. Performance analysis and comparison of dual-hop amplify-and-forward relaying over mixture Gamma and generalized-$K$ fading channels. Proc. Int. Conf. on Wireless Communications & Signal Processing, p.1-6. http://dx.doi.org/10.1109/WCSP.2013.6677092

Gradshteyn, I., Ryzhik, I., 2007. Table of Integrals, Series, and Products (7th Ed.) Academic Press, USA.

Jiang, Y., Zhu, J., Zou, Y., 2015. Secrecy outage analysis of multi-user multi-eavesdropper cellular networks in the face of cochannel interference. *Dig. Commun. Netw.*, **1**(1):68-74. http://dx.doi.org/10.1016/j.dcan.2015.02.002

Jung, J., Lee, S.R., Park, H., *et al.*, 2013. Diversity analysis over composite fading channels using a mixture Gamma distribution. Proc. IEEE Int. Conf. on Communications, p.5824-5828. http://dx.doi.org/10.1109/ICC.2013.6655526

Jung, J., Lee, S.R., Park, H., *et al.*, 2014. Capacity and error probability analysis of diversity reception schemes over generalized-$K$ fading channels using a mixture Gamma distribution. *IEEE Trans. Wirel. Commun.*, **13**(9):4721-4730. http://dx.doi.org/10.1109/TWC.2014.2331691

Laourine, A., Alouini, M.S., Affes, S., *et al.*, 2009. On the performance analysis of composite multipath/ shadowing channels using the $\mathcal{G}$-distribution. *IEEE Trans. Commun.*, **57**(4):1162-1170. http://dx.doi.org/10.1109/TCOMM.2009.04.070258

Lei, H., Gao, C., Ansari, I., *et al.*, 2015a. On physical layer security over SIMO generalized-$K$ fading channels. *IEEE Trans. Veh. Technol.*, **65**(9):7780-7785. http://dx.doi.org/10.1109/TVT.2015.2496353

Lei, H., Gao, C., Guo, Y., *et al.*, 2015b. On physical layer security over generalized Gamma fading channels.

*IEEE Commun. Lett.*, **19**(7):1257-1260. http://dx.doi.org/10.1109/LCOMM.2015.2426171

Lei, H., Zhang, H., Ansari, I., *et al.*, 2016a. Performance analysis of physical layer security over generalized-$K$ fading channels using a mixture Gamma distribution. *IEEE Commun. Lett.*, **20**(2):408-411. http://dx.doi.org/10.1109/LCOMM.2015.2504580

Lei, H., Zhang, H., Ansari, I., *et al.*, 2016b. Secrecy outage analysis for SIMO underlay cognitive radio networks over generalized-$K$ fading channels. *IEEE Signal Process. Lett.*, **23**(8):1106-1110. http://dx.doi.org/10.1109/LSP.2016.2587323

Liu, H., Zhao, H., Jiang, H., *et al.*, 2016. Physical-layer secrecy outage of spectrum sharing CR systems over fading channels. *Sci. China Inform. Sci.*, **59**:102308. http://dx.doi.org/10.1007/s11432-015-5451-2

Liu, X., 2013. Probability of strictly positive secrecy capacity of the Weibull fading channel. Proc. IEEE Global Communications Conf., p.659-664. http://dx.doi.org/10.1109/GLOCOM.2013.6831147

Pan, G., Tang, C., Zhang, X., *et al.*, 2016. Physical-layer security over non-small-scale fading channels. *IEEE Trans. Veh. Technol.*, **65**(3):1326-1339. http://dx.doi.org/10.1109/TVT.2015.2412140

Prudnikov, A.P., Brychkov, Y.A., Marichev, O.I., 1992. Integrals and Series, Volume 2: Special Functions. Gordon and Breach Science Publishers, New York.

Shankar, P.M., 2004. Error rates in generalized shadowed fading channels. *Wirel. Pers. Commun.*, **28**(3):233-238. http://dx.doi.org/10.1023/B:wire.0000032253.68423.86

Stuber, G.L., 2011. Principles of Mobile Communication. Springer Science & Business Media, New York.

Wang, L., Elkashlan, M., Huang, J., *et al.*, 2014. Secure transmission with antenna selection in MIMO Nakagami-$m$ fading channels. *IEEE Trans. Wirel. Commun.*, **13**(11):6054-6067. http://dx.doi.org/10.1109/TWC.2014.2359877

Yadav, S., Upadhyay, P.K., 2013. Performance analysis of two-way AF relaying systems over cascaded generalized-$K$ fading channels. Proc. National Conf. on Communications, p.1-5. http://dx.doi.org/10.1109/NCC.2013.6487901

Yang, N., Wang, L., Geraci, G., *et al.*, 2015. Safeguarding 5G wireless communication networks using physical layer security. *IEEE Commun. Mag.*, **53**(4):20-27. http://dx.doi.org/10.1109/MCOM.2015.7081071

Zou, Y., Wang, X., Shen, W., 2013. Optimal relay selection for physical-layer security in cooperative wireless networks. *IEEE J. Sel. Areas Commun.*, **31**(10):2099-2111. http://dx.doi.org/10.1109/JSAC.2013.131011

Zou, Y., Champagne, B., Zhu, W.P., *et al.*, 2015a. Relay-selection improves the security-reliability trade-off in cognitive radio systems. *IEEE Trans. Commun.*, **63**(1):215-228. http://dx.doi.org/10.1109/TCOMM.2014.2377239

Zou, Y., Zhu, J., Wang, X., *et al.*, 2015b. Improving physical-layer security in wireless communications using diversity techniques. *IEEE Netw.*, **29**(1):42-48. http://dx.doi.org/10.1109/MNET.2015.7018202

# Appendix: Proof of Lemma 2

We derive the asymptotic CDF from the SNR of a single branch of the main channel. The PDF of $\gamma_{D,j}$ in the form of the MG distribution is expressed by (Atapattu *et al.*, 2011; Lei *et al.*, 2016a)

$$f_{D,j}(\gamma) = \sum_{s=1}^{L} \alpha_{D,s} y^{m_D-1} \exp(-\varsigma_{D,s} y). \qquad \text{(A1)}$$

Using Eq. (3.351.1) in Gradshteyn and Ryzhik (2007), we obtain the CDF of $\gamma_{D,j}$ as

$$F_{D,j}(\gamma) = \sum_{s=1}^{L} \alpha_{D,s}(\varsigma_{D,s})^{-m_D} \Upsilon(m_D, \varsigma_{D,s}\gamma). \quad \text{(A2)}$$

Using Eq. (8.352.6) in Gradshteyn and Ryzhik (2007), we have

$$\Upsilon(m_D, \varsigma_{D,s}\gamma) = (m_D - 1)! \left( 1 - \exp(-\varsigma_{D,s}\gamma) \right. $$
$$\left. \cdot \sum_{n=0}^{m_D-1} \frac{(\varsigma_{D,s}\gamma)^n}{n!} \right). \qquad \text{(A3)}$$

When $\bar{\gamma}_D \to \infty$, we have $\Xi_D = \dfrac{m_D k_D}{\bar{\gamma}_D} \to 0$ and $\varsigma_{D,j} = \dfrac{\Xi_D}{t_j} \to 0$. Using the Taylor series expansion truncated to the $l$th order given by $\exp(x) = \sum_{n=0}^{l} \dfrac{x^n}{n!} + O(x^l)$, we obtain

$$\sum_{n=0}^{m_D-1} \frac{(\varsigma_{D,s}\gamma)^n}{n!} = \exp(\varsigma_{D,s}\gamma) - \frac{(\varsigma_{D,s}\gamma)^{m_D}}{m_D!} + O(\gamma^{m_D}).$$
$$\text{(A4)}$$

Substituting Eq. (A4) into Eq. (A3), we have

$$\Upsilon(m_D, \varsigma_{D,s}\gamma) = \frac{(\varsigma_{D,s}\gamma)^{m_D}}{m_D} + O(\gamma^{m_D}). \quad \text{(A5)}$$

Substituting Eq. (A5) into Eq. (A2), the asymptotic CDF of $\gamma_{D,j}$ is obtained by

$$F_{D,j}^{\infty}(\gamma) = \frac{\lambda}{m_D} \gamma^{m_D}, \qquad \text{(A6)}$$

where $\lambda = \sum_{s=1}^{L} \alpha_{D,s}$. Then the asymptotic PDF of $\gamma_{D,j}$ is expressed as

$$f_{D,j}^{\infty}(\gamma) = \lambda \gamma^{m_D-1}. \qquad \text{(A7)}$$

The moment generating function (MGF) of $\gamma_{D,j}$ is expressed as

$$M_{D,j}^{\infty}(\gamma) = \lambda \Gamma(m_D) s^{-m_D}. \qquad \text{(A8)}$$

Based on Eq. (3), we obtain the MGF of $\gamma_D$ as

$$M_D^{\infty}(\gamma) = A^{N_D}(\Gamma(m_D))^{N_D} s^{-m_D N_D}. \quad \text{(A9)}$$

Based on the relationship between PDF and MGF, we obtain the asymptotic PDF and CDF of $\gamma_D$ as Eqs. (8) and (9), respectively.